Atmospheric Research 94 (2009) 10–18

Contents lists available at ScienceDirect

Atmospheric Research

journal homepage: www.elsevier.com/locate/atmos

Investigating a nonlinear characteristic of El Niño events by conditional nonlinear optimal perturbation

Wansuo Duan *, Feng Xue, Mu Mu

LASG, Institute of Atmospheric Physics, Chinese Academy of Sciences, Beijing 100029, China

ARTICLE INFO

Article history:
Received 4 March 2008
Received in revised form 22 July 2008
Accepted 4 September 2008

Keywords:
ENSO model
Nonlinearity
Optimal perturbation
Strong El Niño events

ABSTRACT

We use the approach of conditional nonlinear optimal perturbation (CNOP) to investigate the optimal precursory disturbances in a theoretical El Niño-Southern Oscillation (ENSO) model and then an intermediate model. By exploring the dynamical behaviors of the El Niño events caused by these CNOP-type precursors, a characteristic for this kind of theoretical El Niño events is shown, i.e., the stronger El Niño events tend to decay faster and have shorter durations of the decaying phase. By examining the observed El Niño events, it is found that the Niño-3.4 SSTA are more potential than the Niño-3 SSTA in illustrating the decaying characteristic of the theoretical El Niño events. In particular, it is the Niño-3.4 indices for the strong El Niño events during 1981–2007 that roughly show the decaying characteristic. Based on the physics of the theoretical model, the mechanism responsible for the above decaying characteristic of strong El Niño events is explored. The analysis demonstrates that the property of the stronger El Niño event decaying faster can be realized only through the linear dynamics with the combined effects of the rising of thermocline and the mean upwelling, but that of the stronger El Niño event having a shorter duration of the decaying phase results from a nonlinear mechanism. It is shown that the nonlinearity related to the anomalous temperature advection in the tropical Pacific shortens the duration of the decaying phase for El Niño event. The stronger the El Niño event, the stronger the nonlinearity, then the more considerable the suppressing of the nonlinearity on the duration of the decaying phase for El Niño event. This explains why the stronger El Niño events have shorter durations of the decaying phase. Also, this sheds light on why the observed strong El Niño events are more likely to show this characteristic.

© 2008 Elsevier B.V. All rights reserved.

1. Introduction

El Niño-Southern Oscillation (ENSO) is inherently caused by interactions between the atmosphere and the ocean in the tropical Pacific (Bjerknes, 1969), which is the most prominent interannual signal in the climate system and has large effects on the weather, even far outside the Pacific basin (Horel and Wallace, 1981; Fracdrich, 1994; Dijkstra, 2005). It is therefore very important to simulate and predict ENSO (Latif et al., 1998; Kirtman et al., 2002; Chen et al., 2004). To achieve them, a pivotal step is to understand ENSO (Neelin, 1991; Wang and Fang, 1996; Jin, 1997; Wang, 2001), where it is necessary to reveal the features of ENSO and to explore their physics (Philander, 1990; Moore and Kleeman, 1996).

Several ENSO features were found. El Niño events occur irregularly at intervals of roughly 2–7 years, although the average is about 3–4 years (Quinn et al., 1987). They typically last 12–18 months, and are accompanied by swings in the Southern Oscillation (Bjerknes, 1969), an interannual mass exchange between the Eastern (Asian–Australia monsoon region) and Western (Pacific trade wind region) Hemispheres (Walker, 1924). Mature phases of warm episodes tend to occur in boreal winter (Mitchell and Wallace, 1996). Furthermore,

* Corresponding author. Tel.: +86 010 82995302; fax: +86 010 82995172.
E-mail address: duanws@lasg.iap.ac.cn (W. Duan).

0169-8095/$ – see front matter © 2008 Elsevier B.V. All rights reserved.
doi:10.1016/j.atmosres.2008.09.003

for most ENSO warm events, there occur with a deepening in the east and a shallowing in the west of the thermocline along the equator, and a phase leading of the thermocline transition to SST prior to the peak of the ENSO event (Wang and Fang, 1996; Duan et al., 2004). Usually, the persistence of the Southern Oscillation breaks down during boreal spring; meanwhile, the weakest persistence of ENSO arises in this season (Webster and Yang, 1992; Clarke and Van Gorder, 1999; Mu et al., 2007a,b). Also the transition of ENSO from a cold event to a warm one occurs almost in boreal spring, or vice versa (Mitchell and Wallace, 1996). Especially, the ENSO events after 1976 climate shift shows a prominent characteristic with the amplitude asymmetry between El Niño and La Nina. Many researches demonstrated that the ENSO asymmetry is a nonlinear characteristic of ENSO (An and Jin, 2004; Duan and Mu, 2006; Duan et al., 2008).

Recently, Duan et al. (2004) used the approach of conditional nonlinear optimal perturbation (CNOP) to investigate the nonlinear characteristic of initial anomalies that evolve into an ENSO event most probably. They showed that the nonlinearity enhances the El Niño caused by CNOP-type initial anomalies, which, however, focuses on the growth phase of the ENSO events. In this paper, attentions are further paid to the decaying phase of the ENSO events caused by this kind of optimal precursory disturbances. A feature for El Niño decaying phase is shown: the stronger El Niño events tend to have shorter durations of the decaying phase, which implies that the stronger El Niño events decay faster, that is, the stronger El Niño events have a larger amplitude of decaying per unit time. Then a number of questions need to be addressed. First, is there any observational evidence showing this feature? Second, which process is essential for this feature? Third, what is the role of the nonlinearity in this feature?

The paper is organized as follows. The approach of CNOP is reviewed in the next section. In Section 3, we compute the optimal precursory disturbances of El Niño events in the theoretical model of Wang and Fang (1996; WF96) and then the intermediate model of Zebiak and Cane (1987; ZC). The dynamical behaviors of these precursory disturbances are investigated and the decaying characteristic of El Niño events is demonstrated in this section. In Section 4, we use the observational data to examine the applicability of the decaying characteristic for theoretical El Niño events. And in Section 5, an explanation is presented based on the WF96 model. We summarize the main results in Section 6 and discuss them in Section 7.

2. Conditional nonlinear optimal perturbation

We write the evolution equations for the state vector w, which may include surface current, thermocline depth, and SST, etc., into a nonlinear model:

$$w(t) = M_t(w_0), \tag{2.1}$$

where w_0 is an initial value of the model, and M_t is the "propagator" that "propagates" the initial value w_0 to the future time τ. If u_0 is an initial perturbation superimposed on a reference state $U(t)$, which is a solution to the nonlinear model and satisfies $U(t)=M_t(U_0)$ (U_0 is the initial value of the reference state), the evolution of u_0 can be obtained by

$$u(t) = M_t(U_0 + u_0) - M_t(U_0). \tag{2.2}$$

For a chosen norm $\|\cdot\|$, an initial perturbation $u_{0\sigma}$ is called CNOP, if and only if

$$J(u_{0\sigma}) = \max_{\|u_0\|\le\sigma} \|M_\tau(U_0 + u_0) - M_\tau(U_0)\|, \tag{2.3}$$

where $\|u_0\|\le\sigma$ is an initial constraint defined by the norm $\|\cdot\|$ and J is the objective function.

CNOP is the initial perturbation that satisfies the prescribed constraint and has the largest nonlinear evolution at time τ (Mu et al., 2003; Mu and Duan, 2003). CNOP is related to the propagator (numerical model M_τ). For the different time intervals $[0,\tau]$, the numerical model could have different outcomes at the future time τ, which may cause the different properties of the objective functions J and could then yield different CNOPs. That is, the CNOPs may be dependent of the time intervals. CNOPs can be computed by using the sequential quadratic programming (SQP) solver (Powell, 1982). This solver is often used to solve the nonlinear minimization problems with equality or/and inequality constraint condition.

In ENSO predictability studies, it is important to find out the initial patterns that evolve into ENSO events most probably and to explore their nonlinear physics (Moore and Kleeman, 1996; Thompson, 1998; Duan et al., 2004). CNOP superimposed on the climatological background state can guarantee this optimal initial pattern due to its maximum nonlinear evolution at the prediction time (Mu et al., 2003; Duan et al., 2004). In other words, CNOP has the highest likelihood to evolve into an El Niño event and acts as the optimal precursor for this El Niño event. CNOP approach can be used to identify the effect of nonlinearities. Along this thinking, CNOP method has been applied to study the nonlinear asymmetry of El Niño and La Niña amplitudes (Duan and Mu, 2006; Duan et al., 2008). In this paper, we will apply the CNOP approach in the theoretical WF96 model and then the intermediate ZC model to explore the decaying behaviors of El Niño events caused by CNOP-type precursors, in attempt to revealing the effect of nonlinearity on the decaying behaviors of El Niño events.

3. Results

We first perform numerical experiments to the theoretical WF96 model and then the intermediate ZC model. A common feature for the model El Niño events is demonstrated, that is, the stronger El Niño events decay faster and have shorter durations of the decaying phase.

3.1. Theoretical model results

The WF96 model has been used in the theoretical studies of ENSO dynamics and predictability (Wang and Fang, 1996; Wang et al., 1999; Duan et al., 2004, 2008; Duan and Mu, 2006; Mu et al., 2007b). The model consists of two dimensionless equations. One describes the evolution of sea surface

temperature anomaly (SSTA), T, in Niño-3 region; and the other depicts the variation of thermocline depth anomaly, h.

$$\begin{cases} \dfrac{dT}{dt} = a_1 T - a_2 h + \sqrt{\dfrac{2}{3}} T(T - \gamma h), \\ \dfrac{dh}{dt} = b(2h - T), \end{cases} \tag{3.1}$$

where $a_1 = \bar{T}_z + \bar{T}_x - \alpha_s$, $\alpha_2 = \mu \bar{T}_x$, $b = (2\alpha)/(p(1-3\alpha^2))$, $\gamma = \mu + \gamma_1$ and $p = (1 - H_1/H)(L_0/L_s)^2$. The characteristic scales of SSTA and thermocline depth anomaly are 2.0 °C and 50 m [WF96], respectively. The expressions $\bar{T}_z T$, $\bar{T}_x(T - \mu h)$, and $-\alpha_s T$ are linear terms in the temperature equation that come from the vertical advection by the anomalous upwelling of the mean ocean temperature ($w\bar{T}_z$), the vertical advection by the mean upwelling of the anomalous ocean temperature ($\bar{w}T_z$), and the linear damping. The coefficients a_1 and a_2 involve basic state parameters $\bar{T}_x$ and $\bar{T}_z$, which characterize, respectively, the mean temperature difference between the equatorial eastern and western basins and between the mixed-layer and subsurface-layer water. These basic state parameters can be time-dependent, reflecting the climatological annual cycle of the basic state. The quadratic term in temperature equation is deduced from the anomalous temperature advection by anomalous upwelling of the anomalous temperature. The linear terms in $h-$Eq depict the effect of equatorial waves on thermocline adjustment ($2bh$) and the effect of the wind forcing ($-bT$). Some nondimensional coupling parameters are presented in this model [WF96]: α is the air–sea coupling coefficient, μ measures the degree of coupling between thermocline fluctuation and SST, and γ_1 represents the contribution of the horizontal temperature advection by anomalous zonal currents to local SST variation. There are also some basic parameters in the WF96 model: the Newtonian cooling coefficient α_s, the mean depth of the thermocline H, and the depth of the mixed layer H_1, the oceanic Rossby radius of deformation L_0, and the Ekman spreading length scale L_s. The typical values of these parameters are listed in Table 1 [WF96].

Let $\boldsymbol{u}_0$ be an initial anomaly of the WF96 model. Then the optimization problem related to CNOP can be defined as follows.

$$J(\boldsymbol{u}_{0\delta}) = \max_{||\boldsymbol{u}_0|| \le \delta} |T(\tau)|, \tag{3.2}$$

where $T(\tau)$ is the evolution of model SSTA obtained by integrating the WF96 model from 0 to τ with the initial value u_0. Thus, $J(\boldsymbol{u}_{0\delta})$ describes the maximum evolution of SSTA at prediction time τ. By solving this optimization problem, the optimal initial perturbations satisfying the constraint $||\boldsymbol{u}_0|| \le \delta$, i.e. CNOPs, $\boldsymbol{u}_{0\delta}$, can be found. These CNOPs are initial anomalies in the WF96 model and represent the optimal precursors for ENSO (Duan et al., 2004).

We choose the norm $||\boldsymbol{u}_0|| = \max\{|T_0|, |h_0|\}$ to measure the magnitude of initial anomalies, where T_0 and h_0 are the initial values of nondimensional SSTA and thermocline depth anomaly. In the WF96 model, if nondimensional $T \ge 0.25$ (dimensional 0.5 °C) persists for more than three months, it is regarded as an El Niño event. Considering this standard of El Niño onset, the initial anomalies related to CNOPs are constrained to $||\boldsymbol{u}_0|| \le \delta$ with $\delta \in [0.11, 0.20]$, where the positive real numbers 0.11 and 0.20 indicates the dimensional 0.22 °C and 0.4 °C, respectively. This constraint condition guarantees that the involved initial anomalies do not have the magnitudes larger than the critical value 0.25 (dimensional 0.5 °C), but have the potential for evolving to El Niño events.

Table 1
The values of the model parameters.

A	μ	γ_1	α_s	H	H_1	L_0	L_s
0.0225	1.315	0.0848	$(125\ \text{day})^{-1}$	150 m	50 m	300 km	338 km

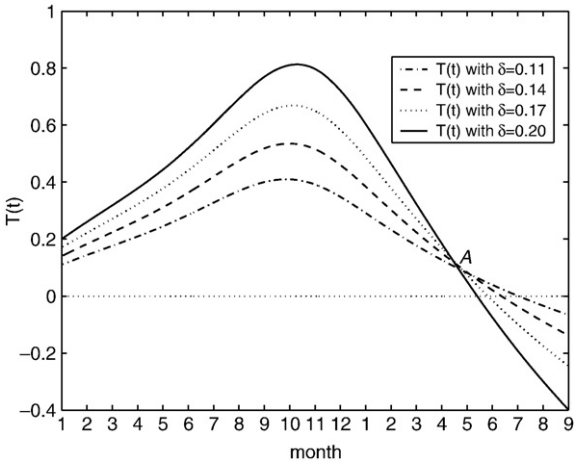

Fig. 1. SSTA component (nondimensional) of the evolutions of the CNOP-type initial anomalies (δ,δ) corresponding to (T, h) in the WF96 model, where δ denotes the magnitude of initial anomalies. The lines represent the SSTA for the model El Niño events with different intensities, respectively. The larger the initial anomalies, the stronger the El Niño events. The stronger model El Niño has a shorter duration of the decaying phase, where the duration of the decaying phase is referred to the time interval between the timing of the peak of the event and the subsequent zero-crossing time.

With the above constraint condition, the optimization problem (3.2) is solved for the time intervals $\tau = 3$, 6, 9, 12 months with initial times as January, February, …, December, respectively. It is shown that there exist a CNOP (δ,δ) of the annual cycle for the time intervals 3 and 6 months, and a CNOP $(-\delta,\delta)$ for the time intervals 9 and 12 months. Furthermore, whatever the initial times are, these CNOPs have similar dynamical behaviors. For simplicity, we use the CNOPs with initial time as January to describe the results. In the following, we first investigate the dynamics of the CNOP-type initial anomalies (δ, δ) with different values of δ.

For a given value of δ, the CNOP, (δ, δ), means an initial anomaly pattern that has a positive SSTA with magnitude δ and a positive thermocline displacement with magnitude δ. To study the dynamics of these CNOP-type initial anomalies, we plot in Fig. 1 the SSTA components of the evolutions of the optimal initial anomalies (δ,δ) with $\delta = 0.11$, 0.14, 0.17, 0.20, respectively. It is shown that for a prescribed δ, the corresponding CNOP evolves into a positive SSTA and attains a peak value, then gradually decays with time, bearing a resemblance with the observed El Niño events. For convenience, we call them model El Niño events. As can be seen, the larger the CNOPs in terms of the chosen norm, the stronger the model El Niño events induced by these CNOPs. Furthermore, the stronger El Niño events tend to decay faster and

have shorter durations of the decaying phase, where the duration of the decaying phase for El Niño is referred to the time interval between the timing of the peak of the event and the subsequent zero-crossing time.

We also investigate the dynamical behavior of the initial anomalies $(-\delta,\delta)$. The results demonstrate this property of El Niño, too. The difference is that the El Niño caused by $(-\delta,\delta)$ persist a longer time than those caused by (δ,δ). For simplicity, we omit the details here. No matter what it is, the property that the stronger El Niño decay faster and have shorter durations of the decaying phase is a common feature of the model El Niño events caused by CNOP-type initial anomalies, which has been ignored in the previous studies related to the applications of CNOP in ENSO studies (Mu et al., 2003, 2007a,b; Mu and Duan, 2003; Duan et al., 2004, 2008; Duan and Mu, 2006).

We note that the WF96 model is a highly simplified one and cannot describe a complete ENSO; furthermore, the robustness of the results needs to be established in more realistic models. Next, we will use the intermediate ZC model to investigate the decaying behaviors of El Niño events and to verify the results of the WF96 model.

3.2. Intermediate model results

As the first dynamical coupled model used for ENSO prediction, the ZC model has been a benchmark in ENSO community for over two decades. It is composed of a Gill-type steady-state linear atmospheric model and a reduced-gravity oceanic model. The atmospheric circulation is forced by a heating anomaly which depends on SST anomaly and moisture convergence whereas the oceanic circulation is driven by surface wind. The SST is determined by the fully nonlinear thermodynamics in a surface mixed layer and by the linear dynamics through thermocline fluctuation. The ZC model may describe the essential physics of ENSO and has been used in the predictions and study of ENSO extensively, thus provides a convenient tool for investigating the decaying behaviors of ENSO.

We construct a cost function to measure the evolution of initial anomalies, which is similar to that in Section 3.1. Then the optimal precursors of El Niño, CNOPs, can be obtained by solving

$$J(\boldsymbol{u}_{0\delta}) = \max_{||\boldsymbol{u}_0||_a \le \delta_{ZC}} ||\boldsymbol{T}(\tau)||_b, \tag{3.3}$$

where $\boldsymbol{u}_0 = (w_1^{-1}\boldsymbol{T}_0, w_2^{-1}\boldsymbol{h}_0)$ is the nondimensional initial SSTA and thermocline depth anomaly, w_1 and w_2 denote the characteristic scales of dimensional SSTA and thermocline depth anomaly and are taken as those of the WF96 model, i.e., $w_1 = 2.0$ °C and $w_2 = 50$ m. The condition $||\boldsymbol{u}_0||_a \le \delta$ is the constraint defined by the norm $||\boldsymbol{u}_0||_a = \sqrt{\sum_{i,j}\left\{\left(w_1^{-1}T_{0i,j}\right)^2 + \left(w_2^{-1}h_{0i,j}\right)^2\right)\right\}}$, where (i,j) represents a grid point in the region from 129.375E to 84.375W by grid spacing of 5.625° and from 19S to 19N by grid spacing of 2°. Variables $T_{0i,j}$ and $h_{0i,j}$ denote the dimensional SST and thermocline depth anomalies at grid point (i,j). The evolutions of these initial anomalies are measured by the norm $||\boldsymbol{T}(\tau)||_b = \sqrt{\sum_{i,j}\left(w_1^{-1}T_{i,j}(\tau)\right)^2}$, and $T_{i,j}(\tau)$ is obtained by integrating the ZC model from time 0 to τ with a proper initial condition u_0.

For $\delta_{ZC} \in [0.6,1.0]$, the optimal perturbations satisfying the condition $||u_0||_a \le \delta_{ZC}$, i.e., CNOPs, are obtained, which are most likely to evolve into El Niño events in the ZC model. In numerical experiments, we compute the CNOPs of the ZC model with the same time intervals as those of the WF96 models. In illustrating the decaying characteristic of the El Niño events, these CNOPs show similar behaviors. To describe the results, we plot in Fig. 2 the Niño-3 SSTA for the El Niño events caused by the CNOPs with initial time as January. It is shown that the larger the CNOPs in terms of the chosen norm $||\cdot||_a$, the stronger the El Niño events caused by them. Furthermore, these model El Niño events tend to peak in December of the year and then decay. In the decaying phase, they possess such property as that the strong El Niño events are earlier than the weak ones to attain the SSTA normal state and have shorter durations of the decaying phase. It is obvious that the results of the ZC model support those of the theoretical WF96 model.

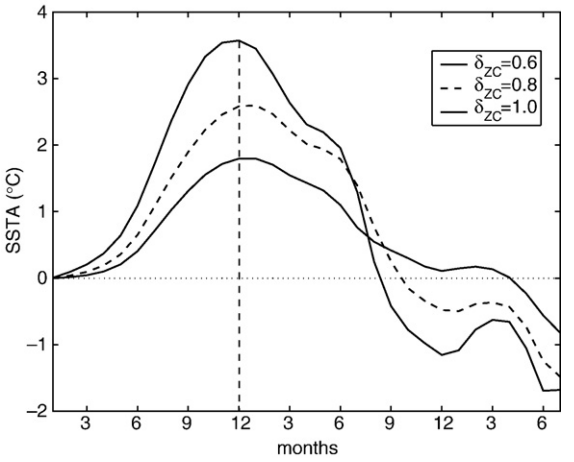

Fig. 2. SSTA component (Niño-3 indices; dimensional) of the evolutions of the CNOP-type initial anomalies (T, h) in the ZC model. The stronger model El Niño has a shorter duration of the decaying phase.

4. Data analysis

The theoretical results have demonstrated that the El Niño events caused by CNOP-type initial anomalies either in the WF96 model or in the ZC model have a common feature with the stronger El Niño events decaying faster and having shorter durations of the decaying phase. To examine if the observed El Niño events show this characteristic, we choose the anomalous monthly mean SST data from November 1981 to September 2007. During this period, six major El Niño events occurred with different intensities. These El Niño events include the 82/83, 86/87, 91/92, 97/98, 02/03, and 06/07 El Niño events. They all experience a growth phase, a mature phase, and a decaying phase. Furthermore, these El Niño events tend to warm in northern spring and peak at the end of the year except for the 86/87 El Niño event. For the decaying phases of these El Niño events, we investigate the time-dependent evolutions of the Niño-3 and Niño-3.4 indices, respectively. It is found that the Niño-3.4 indices for the observed El Niño events are more potential than Niño-3 indices in illustrating the decaying characteristic of the theoretical El Niño events.

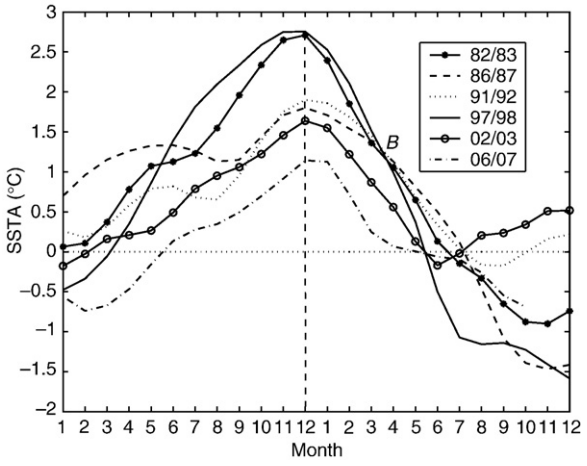

Fig. 3. Time-dependent evolutions of the observed SSTA (Niño-3.4 indices) for the El Niño events during 1981–2007. These El Niño are 82/83, 86/87, 91/92, 97/98, 02/03, and 06/07 events, respectively. The vertical dashed-lines indicates the timing of the peaks for El Niño events.

Fig. 3 plots the time-dependent evolutions of SSTA averaged over Niño-3.4 region by moving their peaks to the same time (i.e. December), where the SSTA series are smoothed by a five-point Gaussian filter. It is noticed that during the decaying phases, these El Niño events behave in difference (Fig. 3). Practically, when they decay, they prefer to converge at a point "B" except for the weak 02/03 and 06/07 El Niño events. Through this point, these four strong El Niño events have a reversed sequence in amplitude. Consequently, the stronger the El Niño event is, the earlier the corresponding SSTA attain the normal state. That is to say, the stronger El Niño events tend to have shorter durations of the decaying phase. Then the stronger El Niño events decay faster.

For the observed El Niño events of 1950–1980, we also investigate their decaying phases. It is found that they have not the above decaying characteristic. However, some typical El Niño events among them tend to feature that the stronger El Niño events possess longer duration of the decaying phase. This is different from the decaying characteristic of the El Niño events after 1970s. This difference indicates that the ENSO may have different dynamical regimes in different decades. Both the theoretical WF96 model and the intermediate ZC model, under the condition of the present model parameter values, may be applicable for describing the dynamical regime related to the post-1970s.

From above discussions, it is shown that the Niño-3.4 indices for the strong El Niño events after 1970s roughly show the decaying characteristic of the theoretical El Niño events in the WF96 and ZC models, that is, the stronger El Niño events decay faster and have shorter durations of the decaying phase. Then what mechanism causes this characteristic? Which process is responsible for it?

5. Interpretations

The physical explanation of fundamental characteristics for ENSO requires a theoretical model (Wang and Fang, 1996; Jin, 1997; Wang, 2001; Wang et al., 1999; Tziperman et al., 1994). As shown in the previous sections, the WF96 model is a theoretical ENSO model and particularly captures the characteristic that the stronger El Niño events tend to decay faster and have shorter durations of the decaying phase. Furthermore, its results can be supported by those of the realistic ZC model. Therefore, we use the theoretical WF96 model to address the mechanism of the decaying characteristic for the El Niño events.

For the El Niño events in the linearized version of the WF96 model (hereafter as L-WF96 model), we also investigate their decaying behaviors by examining the linear evolutions of the CNOPs. It is found that the stronger El Niño events in the L-WF96 model do not have a shorter decaying phase, but tend to have a larger decaying speed (Fig. 4). This indicates that the property of the stronger El Niño events decaying faster is a characteristic of linear dynamics for the El Niño events, while that of the stronger El Niño events having shorter durations of the decaying phase is nonlinear. Therefore, we will address the physical mechanism from two aspects: one is why the stronger El Niño event decays faster; the other is why the stronger El Niño event has a shorter duration of the decaying phase.

5.1. Why do the stronger El Niño events decay faster?

The decaying of El Niño events attributes to the negative feedback processes that transfer the ENSO from a warm state to a cold one. In the WF96 model, the negative feedback involves two processes: the vertical advection of heat by mean upwelling and the vertical displacement of thermocline due to ocean wave adjustment, both of which are included in the linear dynamics of the WF96 model (i.e., the L-WF96 model). When the warming in the eastern Pacific is sufficiently strong, the above two processes act against the warming and are favorable for the SSTA decaying. First, the warming increases the anomalous vertical temperature difference across the mixed layer base, $T-T_e=T-\mu h$. When this difference is larger than the normal, the vertical advection induced by the mean upwelling, $\bar{T}_x(T-\mu h)$, would suppress the warming.

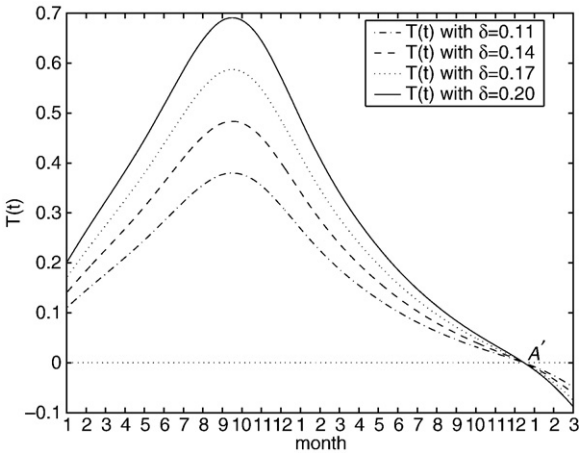

Fig. 4. SSTA components (nondimensional) of the evolutions of CNOP-type initial anomalies (δ,δ) in the L-WF96 model. These El Niño events with different intensities have the same duration of the decaying phase in the L-WF96 model, but the stronger El Niño event decays faster.

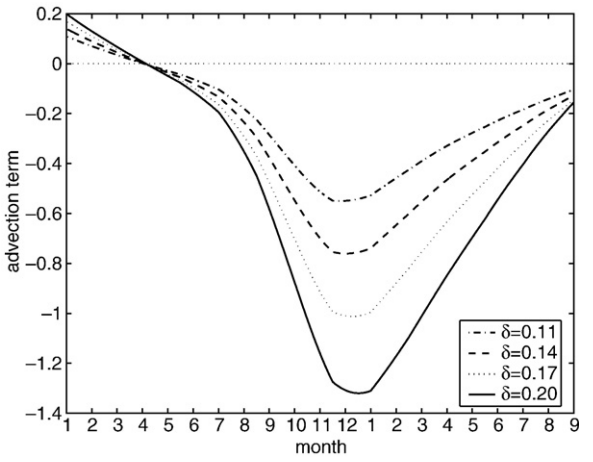

Fig. 5. Temperature advection of heat by mean upwelling, $\bar{T}_x(T-\mu h)$, which correspond to the model El Niño events shown in Fig. 1. δ is the same as in Fig. 1.

Furthermore, the stronger the El Niño event is, the larger the anomalous vertical temperature difference is, then the more significant the suppression of the mean upwelling on El Niño is. For the linear dynamics of the WF96 model, the stronger the El Niño event is, the larger the expression $|\bar{T}_x(T-\mu h)|$ with $\bar{T}_x(T-\mu h)<0$ is (Fig. 5), and the more negative the temperature tendency (dT/dt) in the decaying phase of El Niño is, suggesting that the stronger El Niño event decays faster. Second, the thermocline variation influences directly the SST variation via changing the upwelled water temperature and leads to the SST variation in the eastern Pacific [WF96]. When the warming is sufficiently strong so that $T>2h$ (nondimensional), the thermocline depth in the equatorial eastern Pacific will decrease (b is positive). The rising thermocline would lower the temperature of the water upwelled into the mixed layer and suppress the warming.

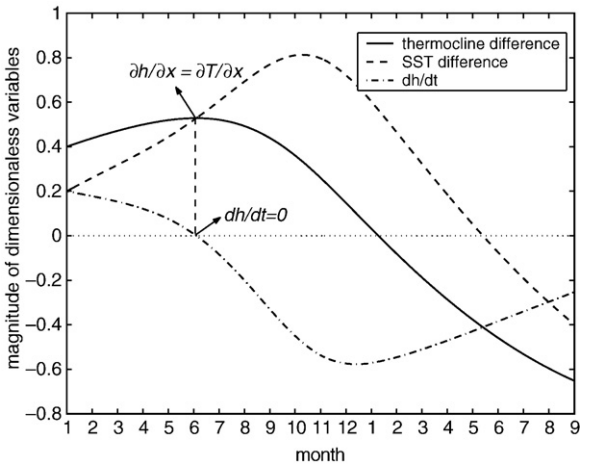

Fig. 6. The anomalous SST difference between equatorial eastern and western Pacific (dashed line), the anomalous thermocline depth difference between them (solid line), and the tendency of the thermocline depth (dh/dt; dash-dot line). These lines correspond to the El Niño event caused by the CNOP (δ, δ) with $\delta=0.20$.

The WF96 model was reduced from the ZC model. In the ZC model, the dynamics of the thermocline depth anomaly h can be approximately described by a simplified dimensionless equation

$$\lambda\frac{\partial}{\partial t}\left[y^2h+\varepsilon\left(\frac{2}{y}\frac{\partial h}{\partial y}-\frac{\partial^2 h}{\partial y^2}\right)\right]-\frac{\partial h}{\partial x}=-\frac{\partial T}{\partial x}, \tag{5.1}$$

where λ measures the importance of the non-Sverdrup balance. Setting $\varepsilon=0$ eliminates the equatorially trapped waves, in which, however, there remains slow divergent motions forced by wind stress and deflected by the Corriolis force and can result in a slow thermocline adjustment. The $h-$Eq is just distilled from Eq. (5.1) by treating the coupled basin mode as an equatorially trapped and symmetric east–west "seesaw". From the expression of Eq. (5.1), it is derived that Eq. (5.1) describes how SST gradients ($\frac{\partial T}{\partial x}$; wind stresses) force the upper ocean and change the thermocline depth. We therefore deduce that in the $h-$Eq of the WF96 model, the term bT qualitatively describes the wind stress forcing, and $2bh$ is proportional to the pressure gradient force associated with the thermocline slope ($\frac{\partial h}{\partial x}$). From the $h-$Eq, it is easily shown that the thermocline variation of the model El Niño events is mainly governed by the competition of the zonal wind stress and the pressure gradient force associated with thermocline slope.

In Fig. 6, we illustrate the anomalous SST difference between equatorial eastern and western Pacific, and the anomalous thermocline depth difference between these two ocean basins. It is shown that with the increasing of the anomalous zonal thermocline depth difference, the anomalous zonal SST difference is also amplified. When the El Niño evolves to be strong enough, the anomalous zonal SST difference will be larger than the anomalous thermocline depth difference. Then the tendency of the thermocline depth becomes negative (i.e. $\frac{dh}{dt}<0$; see Fig. 6 and the $h-$Eq in the WF96 model), which infers that the easterly wind stress will be larger than the pressure gradient force and is favorable for the shoaling of thermocline, suppressing the warming and favoring the decaying of El Niño. It is conceivable that the stronger El Niño event has smaller pressure gradient force related to the thermocline slope, which therefore favors that the stronger El Niño event will have a larger contrast between

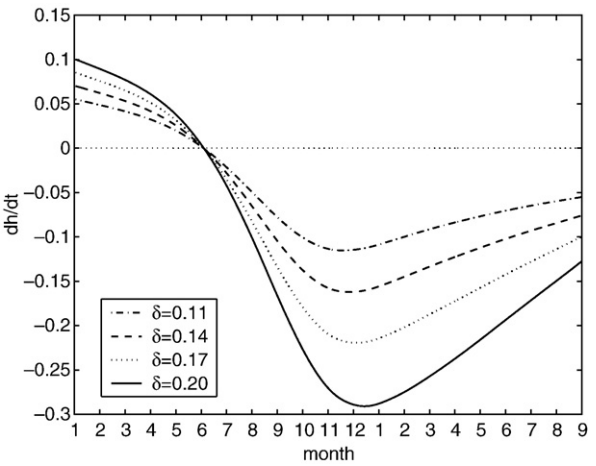

Fig. 7. The tendencies (dh/dt) of the thermocline depth for the model El Niño events shown in Fig. 1, respectively.

the easterly wind stress and the pressure gradient force in its decaying phase. That is to say, the stronger the El Niño events, the larger the values of the thermocline depth tendency $|\frac{dh}{dt}|$ with $\frac{dh}{dt}<0$ (Fig. 7). This suggests that the stronger El Niño event will decay faster.

In the above, we have demonstrated that the vertical temperature advection induced by the mean upwelling and the thermocline displacement provides a negative feedback for the growth of El Niño and favors its decaying. Furthermore, the stronger the El Niño event is, the more significant the contribution of the vertical temperature advection to the decaying of El Niño. The thermocline displacement is mainly governed by the competing effect of the zonal wind stress and the pressure gradient force associated with the thermocline slope, which acts together with the mean upwelling effect to provide a mechanism that the stronger the El Niño event is, the faster it decays.

5.2. Why do the stronger El Niño events have shorter durations of the decaying phase?

The numerical experiments have demonstrated that the property of the stronger El Niño events having shorter durations of the decaying phase could be a nonlinear characteristic of ENSO. Now we explain it based on the theoretical WF96 model.

In the WF96 model, there exists a nonlinear term, $\eta(T,h)=\sqrt{\frac{2}{3}}T(T-\gamma h)$, which is included in the temperature equation and represents the anomalous temperature advection process. The nonlinear effect in the WF96 model originates from this nonlinear term. To measure the effect of this nonlinearity on El Niño, we consider the difference between the nonlinear and linear evolutions of SSTA. For convenience, we denote this difference as Φ. Fig. 8 illustrates these differences (Φ) with the nonlinear evolutions of SSTA minus the linear ones. It is shown that in the decaying phase

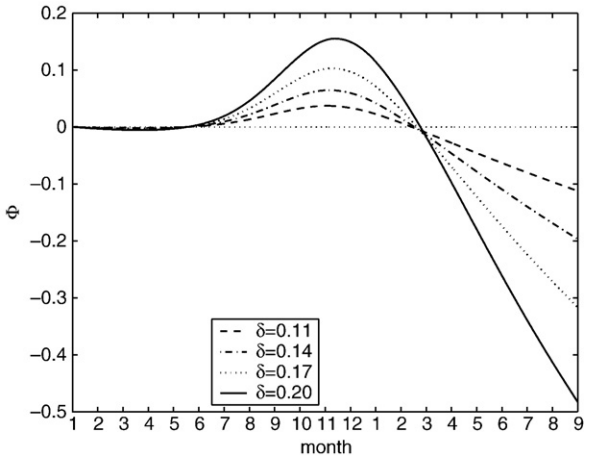

Fig. 8. Differences (Φ) between the nonlinear and linear evolutions of SSTA components in CNOP-type initial anomalies, which correspond to the model El Niño events shown in Fig. 1 and measure the effect of the nonlinearity on the SSTA amplitudes for these model El Niño events. The larger the values of $|\Phi|$, the more considerable the effect of the nonlinearity on SSTA amplitude. The positive (negative) values of Φ indicate that the nonlinearity enhances (suppresses) El Niño.

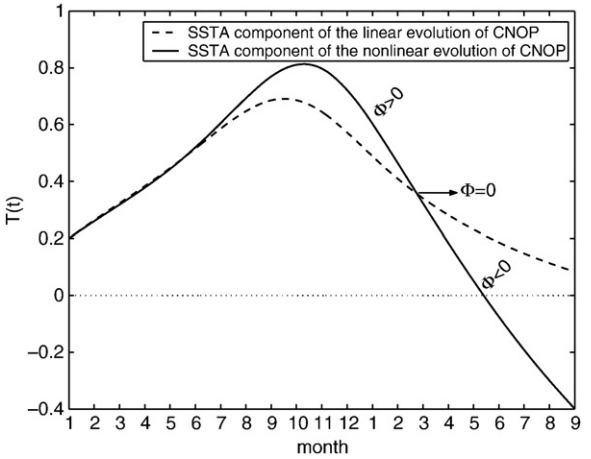

Fig. 9. An example showing the comparison between the El Niño event in the WF96 model and that in the L-WF96 model, where the El Niño events are respectively obtained by integrating the WF96 model and the L-WF96 model with the initial anomaly (δ,δ) ($\delta=0.20$). The time interval in which the El Niño in the WF96 model is stronger (weaker) than that in the L-WF96 model corresponds to $\Phi>0$ ($\Phi<0$), indicating the nonlinearity with $\Phi>0$ ($\Phi<0$) enhances (suppresses) the El Niño.

of El Niño, the differences Φ are first positive, and then develop to be negative. From the temperature equation in the WF96 model, it is derived that the positive (negative) Φ will amplify (decrease) the positive SSTA of El Niño. Fig. 9 illustrates this fact. From Figs. 8 and 9, it is easily shown that the negative Φ in the decaying phase of El Niño is favorable for making SST transition from a positive anomaly to a negative one. This implies that the nonlinearity shortens the duration of the decaying phase for El Niño.

From Fig. 8, it is also shown that the stronger El Niño events have stronger nonlinearities. In particular, when the SSTA decays to be sufficiently small, the differences Φ symbolizing the nonlinearity become negative. Furthermore,

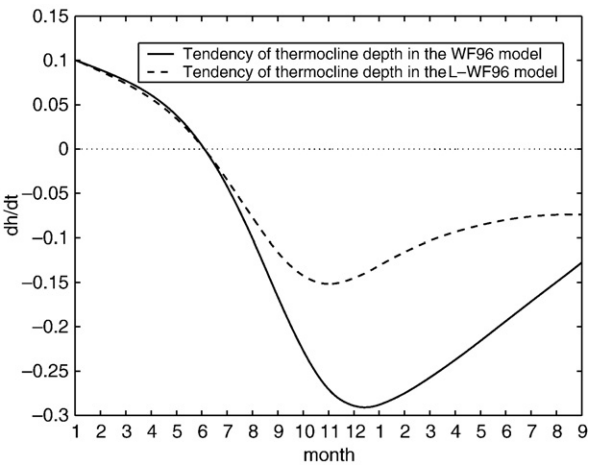

Fig. 10. The tendencies of the thermocline depth corresponding to the El Niño event caused by the CNOP (δ,δ) with $\delta=0.20$. The solid (dashed) line represents the tendency of the thermocline depth in the WF96 model (L-WF96 model). They have significant difference, which indicates the pronounced nonlinear effect on the thermocline variation.

the stronger the El Niño events, the larger the values of the $|\Phi|$ with $\Phi<0$, which implies that in the decaying phase, the stronger El Niño events have a more significant SSTA decreasing caused by the nonlinearities with $\Phi<0$. Then the stronger El Niño events tend to be earlier to attain the SST normal state. That is, the stronger the El Niño event, the shorter the duration of the decaying phase.

On the other hand, one of the key physical processes in the WF96 model that transfers the ENSO from a warm state to a cold one is the upwelling of the subsurface water. In the decaying phase of El Niño events, the rising of the thermocline would lower the temperature of the water upwelled into the mixed layers and induce the SST transition from a positive anomaly to a negative one. Fig. 9 demonstrates that for the same initial anomaly, the El Niño event in the WF96 model is much strong compared to that in the L-WF96 model. This much strong El Niño event amplified by the nonlinearity with $\Phi>0$ (see Figs. 8 and 9) will cause a much small pressure gradient force related to the thermocline slope and induce much large contrast between the easterly wind stress and the pressure gradient force, causing the much large values of the thermocline displacement tendency $\frac{dh}{dt}$ with $dh/dt<0$ (Fig. 10). This indicates that the much fast rising of the thermocline in the WF96 model will lower quickly the temperature of the water upwelled into the mixed layer, which would have much large amplitude to cool the SST, then much favorable for the SST changing from warming to cooling. These comparisons between the WF96 model and the L-WF96 model illustrate that the nonlinearity would shorten the duration of the decaying phase for El Niño events. Furthermore, for the stronger El Niño event, the thermocline variation is affected by the stronger nonlinearity (Fig. 11), which will induce the larger effect of nonlinearity on El Niño decaying, that is, the stronger nonlinearities induced by the stronger El Niño events would more considerably shorten the decaying phase for El Niño. Considering that the durations of the decaying phases for the El Niño events with different intensities are almost the same in the L-WF96 model (see Fig. 4), we obtain that the stronger El Niño events in the WF96 model tend to have shorter durations of the decaying phase due to the nonlinear effect.

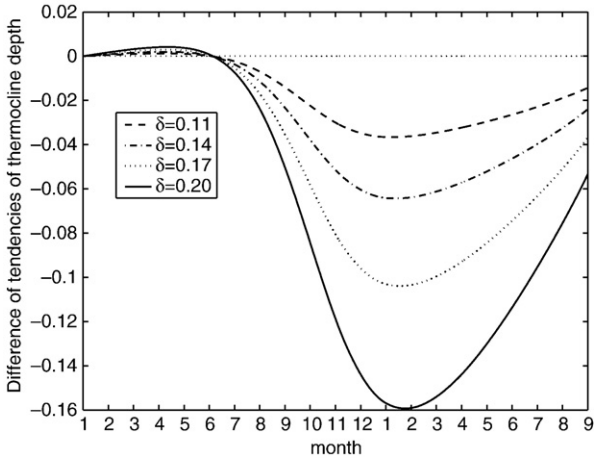

Fig. 11. Differences between the tendencies of the thermocline depth in the WF96 model and those in the L-WF96 model. The lines represent the differences corresponding to the El Niño events shown in Fig. 1. The large (small) differences indicate the strong (weak) effect of nonlinearity on thermocline variations.

This above analysis illustrates that the stronger the El Niño events are, the stronger the nonlinearities are, and the more significant the nonlinearity shortens the durations of the decaying phase for El Niño events. Thus this explains why the stronger El Niño events have shorter durations of the decaying phase. This also shed lights on that why only the observed strong El Niño events roughly show the decaying characteristic of the theoretical El Niño events.

6. Summary

The theoretical WF96 model and the intermediate ZC model have been used to investigate the decaying behaviors of El Niño events by applying CNOP approach in finding the optimal precursory disturbances for ENSO. The results demonstrate that for the El Niño events caused by CNOPs, the stronger El Niño events tend to decay faster and have shorter durations of the decaying phase. By investigating the observed El Niño events, it is found that the Niño-3.4 indices are more potential than the Niño-3 indices in showing the decaying characteristic of the theoretical El Niño events. Practically, the strong El Niño events during 1981–2007 roughly exhibit the decaying characteristic of the theoretical El Niño events.

Based on the theoretical WF96 model, we explored the possible mechanism responsible for the above decaying characteristic of strong El Niño events. The mechanism can be addressed from two aspects: one is that the stronger El Niño events decay faster; the other is that the stronger El Niño events have shorter durations of the decaying phase.

In the former, the property that the stronger El Niño events decay faster can be realized by the linear dynamics of the WF96 model, which is therefore a linear characteristic for El Niño events. In this case, two physical processes play the dominant role. One is the vertical advection of heat by mean upwelling, which suppresses the El Niño and favors its decaying. The stronger El Niño events will have larger anomalous vertical temperature gradients, which acts together with the mean upwelling and advances the decaying of the stronger El Niño. The other is the competing effect of the easterly wind stress and the pressure gradient force associated with the thermocline slope. The stronger El Niño will yield a weaker pressure gradient force and cause a larger difference between the easterly wind stress and the pressure gradient force, which will make the shoaling of thermocline and the El Niño decay faster.

In the latter, the property that the stronger El Niño have shorter durations of the decaying phase results from a nonlinear mechanism. In the WF96 model, there exists a nonlinear term related to the anomalous temperature advection. This nonlinear term is included in the temperature equation, but it affects not only the SSTA evolutions but also the thermocline depth anomaly evolutions. On one hand, the nonlinearity shortens the duration of the decaying phase by suppressing the amplitude of SSTA during the decaying phase. The stronger the El Niño event, the stronger the nonlinearity, then the more considerable the nonlinear effect that the anomalous temperature advection shortens the duration of the decaying phase. On the other hand, the nonlinearity strengthens the El Niño in the former

period of the decaying phase and causes a much small pressure gradient force by affecting the thermocline slope, which induces a much large contrast between the easterly wind stress and the pressure gradient force and causes a much negative tendency of the thermocline depth. The resultant much fast shoaling of the thermocline will be more considerable to lower the temperature of the upwelled water and make the SST in the WF96 model prior to those in the L-WF96 model transition from warming to cooling. Then the nonlinearity shortens the duration of the nonlinearity by affecting the thermocline variations. The stronger El Niño event has stronger nonlinearity, which will have larger amplitude to shorten the duration of the decaying phase for El Niño.

The above results have shown that the strong El Niño events are affected by strong nonlinearities, and the strong nonlinearities cause the short durations of the decaying phase. It is inferred that the decaying characteristic of El Niño demonstrated above attributes to the strong nonlinearities related to the strong El Niño events. That is to say, the above decaying characteristic of El Niño should be subject to the strong El Niño events. Considering that ENSO system has changed from a relatively stable to an unstable oscillating system with strong nonlinearities (An and Jin, 2004; Duan and Mu, 2006, Duan et al., 2008), it is therefore conceivable that only the observed strong El Niño events after 1970s show the decaying characteristic of theoretical El Niño events.

7. Discussion

In this paper, we used the CNOP approach to show the decaying characteristic for El Niño events. This characteristic can also be observed from Fig. 10 in WF96. However, in revealing the effect of nonlinearity on the duration of the decaying phase, the CNOP approach is useful. It suggests that the property of the stronger El Niño events having shorter durations of the decaying phase results from a nonlinear mechanism.

It is of importance to point out the limitations of the results obtained here. In this paper, within the frame of the WF96 model and the ZC model, the results demonstrate the above decaying characteristic of the theoretical El Niño events by Niño-3 indices. In numerical experiments, we attempt to use observed the Niño-3 indices for El Niño events to verify the theoretical results. However, it is found that the Niño-3.4 indices for the observed strong El Niño events are much better than the Niño-3 indices in validating the decaying characteristic of the theoretical El Niño events. It would therefore be a discrepancy between observation and models. Then the results obtained here are limited in the models' ability to simulate the real system. This limitation would compel scientists to improve the models in some aspects. It is expected that better simulations will be possible with more sophisticated models.

Acknowledgements

The authors are grateful to the two anonymous reviewers for their very valuable comments. This work was jointly sponsored by the KZCX3-SW-230 of the Chinese Academy of Sciences, the National Nature Scientific Foundation of China (No. 40505013), and the National Basic Research Program of China (Nos. 2006CB403606 and 2007CB411800).

References

An, S.-I., Jin, F.F., 2004. Nonlinearity and asymmetry of ENSO. J. Climate 17, 2399–2412.
Bjerknes, J., 1969. Atmospheric teleconnections from the equatorial Pacific. Mon. Weather Rev. 97, 163–172.
Clarke, A.J., Van Gorder, S., 1999. The connection between the boreal spring southern oscillation persistence barrier and biennial variability. J. Climate 12, 610–620.
Chen, D., Cane, M.A., Kaplan, A., Zebiak, S.E., Huang, D.J., 2004. Predictability of El Niño over the past 148 years. Nature 428, 733–736.
Dijkstra, H., 2005. Nonlinear Physical Oceanography: A Dynamical Systems Approach to the Large Scale Ocean Circulation and El Niño. Springer, p. 532.
Duan, W.S., Mu, M., Wang, B., 2004. Conditional nonlinear optimal perturbation as the optimal precursors for El Niño-Southern Oscillation events. J. Geophys. Res. 109 (D23105). doi:10.1029/2004JD004756.
Duan, W.S., Mu, M., 2006. Investigating decadal variability of El Niño-Southern Oscillation asymmetry by conditional nonlinear optimal perturbation. J. Geophys. Res. 111 (C07015). doi:10.1029/2005JC003458.
Duan, W.S., Xu, H., Mu, M., 2008. Decisive role of nonlinear temperature advection in El Niño and La Nina amplitude asymmetry. J. Geophys. Res. 113 (C01014). doi:10.1029/2006JC003974.
Fracdrich, K., 1994. An ENSO impact on Europe? A review. Tellus, Ser. A 46, 541–552.
Jin, F.F., 1997. An equatorial ocean recharge paradigm for ENSO. Part I: conceptual model. J. Atmos. Sci. 54, 811–829.
Horel, J.D., Wallace, J.M., 1981. Planetary scale atmospheric phenomena associated with the Southern Oscillation. Mon. Weather Rev. 109, 813–829.
Kirtman, B.P., Shukla, J., Balmaseda, M., Graham, N., Penland, C., Xue, Y., Zebiak, S., 2002. Current status of ENSO forecast skill: A report to the Climate Variability and Predictability (CLIVAR) Numerical Experimentation Group (NEG), CLIVAR Working Group on Seasonal to Interannual Prediction. Clim. Variability and Predictability. Southampton Oceanogr. Cent., Southampton, UK.
Latif, M., Abderson, D., Barnett, T., Cane, M., Kleeman, R., Leetmaa, A., O'Brien, J., Rosati, A., Schneider, E., 1998. A review of the predictability and prediction of ENSO. J. Geophys. Res. 103 (C7), 14375–14393.
Mitchell, T.P., Wallace, J.M., 1996. ENSO seasonality: 1950–78 versus 1979–92. J. Climate 9, 3149–3161.
Moore, A.M., Kleeman, R., 1996. The dynamics of error growth and predictability in a coupled model of ENSO. Q. J. R. Meteorol. Soc. 122, 1405–1446.
Mu, M., Duan, W.S., Wang, B., 2003. Conditional nonlinear optimal perturbation and its applications. Nonlinear Process. Geophys. 10, 493–501.
Mu, M., Duan, W.S., 2003. A new approach to studying ENSO predictability: conditional nonlinear optimal perturbation. Chin. Sci. Bull. 48, 1045–1047.
Mu, M., Xu, H., Duan, W.S., 2007a. A kind of initial errors related to "spring predictability barrier" for El Niño event in Zebiak–Cane model. Geophys. Res. Lett. 34 (L03709). doi:10.1029/2006GL027412.
Mu, Mu, Duan, Wansuo, Wang, Bin, 2007b. Season-dependent dynamics of nonlinear optimal error growth and ENSO predictability in a theoretical model. J. Geophys. Res. 112 (D10113). doi:10.1029/2005JD006981.
Neelin, J.D., 1991. A hybrid coupled general circulation model for El Niño studies. J. Atmos. Sci. 47, 674–693.
Powell, M.J.D., 1982. VMCWD: a FORTRAN subroutine for constrained optimization. DAMTP Report 1982/NA4. University of Cambridge, England.
Philander, S.G., 1990. El Niño, La Nina, and the Southern Oscillation. Academic Press. 289 pp.
Quinn, W.H., Neal, V.T., Antunez de Mayolo, S.E., 1987. El Niño occurrences over the past four and a half centuries. J. Geophys. Res. 92, 14449–14461.
Tziperman, E., Stone, L., Cane, M.A., Jarosh, H., 1994. El Niño chaos: overlapping of resonances between the seasonal cycle and the Pacific ocean–atmosphere oscillator. Science 264, 72–74.
Thompson, C.J., 1998. Initial conditions for optimal growth in a coupled ocean–atmosphere model of ENSO. J. Atmos. Sci. 55, 537–557.
Walker, G.T., 1924. Correlation in seasonal variations of weather IX: a further study of world weather. Mem. Indian Meteor. Dept. 25, 275–332.
Wang, B., Fang, Z., 1996. Chaotic oscillation of tropical climate: a dynamic system theory for ENSO. J. Atmos. Sci. 53, 2786–2802.
Wang, B., Barcilon, A., Fang, Z., 1999. Stochastic dynamics of El Niño-Southern Oscillation. J. Atmos. Sci. 56, 5–23.
Wang, C.Z., 2001. A unified oscillator model for the El Niño-Southern Oscillation. J. Climate 24, 98–115.
Webster, P.J., Yang, S., 1992. Monsoon and ENSO: selectively interactive systems. Quart. J. Roy. Meteor. Soc. 118, 877–926.
Zebiak, S.E., Cane, A., 1987. A model El Niño-Southern oscillation. Mon. Weather Rev. 115, 2262–2278.